Facial Soft-Tissue Asymmetry in 3D Cone Beam Computed Tomography Images of Children with Surgically Corrected Unilateral Clefts

John M. Starbuck, PhD[1], Ahmed Ghoneima, PhD[1], Katherine Kula, DMD[1]

[1]Department of Orthodontics and Oral Facial Genetics, School of Dentistry, Indiana University, Indianapolis, IN 46202

KEY WORDS: soft-tissue depth; facial reconstruction; cleft lip with or without cleft palate

Correspondence to:

John Marlow Starbuck, PhD
Department of Orthodontics and Facial Genetics
Indiana University School of Dentistry
1121 W. Michigan St. DS 250B
Indianapolis, IN 46202
jstarbuc@iu.edu
317-278-1209 (office)
317-278-1438 (fax)

Grant Funding: Indiana University-Purdue University Indianapolis Signature Center Initiative: 3D Imaging of the Craniofacial Complex Center; Jarabak Endowed Professorship

---

Starbuck JM, Ghoneima A, Kula K. Facial soft-tissue asymmetry in three-dimensional cone-beam computed tomography images of children with surgically corrected unilateral clefts. J Craniofac Surg. 2014 Mar;25(2):476–80. http://dx.doi.org/10.1097/SCS.0000000000000619

ABSTRACT

Cleft lip with or without cleft palate (CL/P) is a relatively common craniofacial malformation involving bony and soft-tissue disruptions of the nasolabial and dentoalveolar regions. The combination of CL/P and subsequent craniofacial surgeries to close the cleft and improve appearance of the cutaneous upper lip and nose can cause scarring and muscle pull, possibly resulting in soft-tissue depth asymmetries across the face. We tested the hypothesis that tissue depths in children with unilateral CL/P exhibit differences in symmetry across the sides of the face. Twenty-eight tissue depths were measured on cone beam computed tomography (CBCT) images of unilateral CL/P children (n = 55), aged 7-17 yrs., using Dolphin software (v 11.5). Significant differences in tissue depth symmetry were found around the cutaneous upper lip and nose in unilateral CL/P patients.

Introduction

Human faces exhibit a wide range of variation in facial form and appearance due to various factors including environment, ethnic background, age, gender, and congenital anomalies.[1-3] Human facial morphogenesis occurs during development as several facial prominences fuse and grow harmoniously to produce a functional craniofacial unit.[4] Age-related changes in facial proportions, tissue thickness, and facial appearance occur as individuals grow and throughout senescence.[5-13] Congenital craniofacial anomalies arise when facial prominences fail to fuse or grow in a coordinated fashion and can result in asymmetry affecting the skull and face on a global or local scale.

Cleft lip with or without cleft palate (CL/P) is a relatively common craniofacial birth defect affecting 1 in 1500 children per year.[14-16] CL/P is caused by an embryologic failure of the nasal and maxillary facial prominences to fuse correctly on the 36th or 37th day of gestation and results in asymmetric muscle pull on the nasal septum during osteogenesis of the midface.[17] Archaeological and historical evidence suggest that methods of CL/P surgical correction have existed for at least 1600 years; however, it wasn't until the nineteenth century that these methods began to be employed frequently.[18-20] Today, the lips and alveolus of children with clefts are surgically repaired around the third month of life with the intention of reducing facial stigmata during childhood.[21,22] The combination of congenital clefts and subsequent functional and aesthetic surgical grafts/corrections might result in changes to nasal septum growth, abnormal tooth morphogenesis and eruption patterns, missing or supernumerary teeth, malocclusion, midfacial deficiency, maxillary asymmetry, reductions of nasal airway size, defects in upper lip musculature, and increased mouth breathing.[23-32] These factors can affect facial soft-tissue development and growth by causing scarring, muscle pull, changes to nasal form and function, and thinner and less elastic tissues around the site of surgical repair.[17,33-36]

Morphological asymmetry across the face, and particularly in the nasolabial regions, has previously been reported in CL/P.[17,29,37] Kane and colleagues quantified craniofacial asymmetry in pre-operative infants and found that asymmetry is most extreme near the cleft, but subtle asymmetry is also present in other parts of the face and cranial base.[38] Follow up of 11 month old patients who had undergone primary cleft repair at 3 months revealed that primary surgical repair significantly reduced asymmetry across the face, particularly in the oronasal regions, and provided sufficient tensional forces to mold and improve symmetry of underlying osseous structures.[39] In a longitudinal study investigators found facial oronasal asymmetry in 10-year old unilateral CL/P patients and noted that faces which were more symmetric after primary surgery were more likely to be more symmetric at the age of 10, thereby underscoring the importance of achieving symmetry during the primary cleft repair.[40] Bugaighis and investigators found the most extreme asymmetry near the nasolabial regions of the unilateral CL/P face, but also found asymmetry across the rest of the face, particularly near the orbits.[37] The results from these studies suggest that perturbations to facial morphogenesis and growth can affect the entire craniofacial complex, likely by altering morphological integration of component parts of the face during development.[41] Although it is useful for surgeons to have a complete picture of the relationship between osseous and soft-tissue surgical repair(s), symmetry of unilateral CL/P tissue depths has seldom been investigated.

Three-dimensional (3D) cone beam computed tomography (CBCT) images are useful for assessing the relationship between hard and soft tissue of the face because the relationship between these two tissues is maintained when the image is acquired. The goal of this study is to use 3D CBCT images to determine if craniofacial CL/P tissue depths are symmetric and to localize symmetry differences that are present to specific facial regions. We hypothesize that CL/P facial tissue depths will show differences in symmetry due to the initial congenital cleft or subsequent surgeries aimed at improving aesthetic appearance.

Materials and Methods

3D cone beam computed tomography (CBCT) images (0.3- 0.4 mm voxel size; i-Cat machine, Imaging Sciences International LLC, Hatfield, PA) were acquired from pre-existing orthodontic records at the Indiana University School of Dentistry with IRB approval from the Indiana University Human Subjects Office (Study # 1210009813). CBCT images of children used in this study (n = 55; Table 1) were previously diagnosed with Veau Class III unilateral cleft lip and palate and had undergone at least one surgical correction to repair the lip and alveolus. It was not possible to determine the exact lip and palate surgical protocols used on each patient and it is likely that heterogeneous methods were employed by the different plastic surgeons involved. Due to limitations of sample size no attempt was made to control for ancestry; however, the majority of the sample was Caucasian.

Dolphin Imaging software (v11.5; Chatsworth, CA) was used by the same individual (JMS) on the same computer and monitor to measure tissue depths on coded unilateral CL/P CBCT images. To minimize measurement error, an orientation module in Dolphin was used to standardize the orientation of images by passing a line through orbitale and porion in lateral view, and by passing a line through nasion and pogonion and frontal view. Fourteen soft-tissue depths (Table 2) were measured from each CBCT image on each side of the skull and face (Fig. 1) by placing homologous soft and hard-tissue landmarks and measuring the distance between these points using integrated measurement tools. All statistical testing was conducted using Minitab (v.16.1.0).

During a repeatability study all tissue depths (Table 2) were measured by one investigator (JMS) blinded to the identity of 10 random coded images on three separate occasions with at least 24 hours between each measurement session to minimize memory bias. The intra-class correlation (ICC) coefficient was calculated using a 2-way random ANOVA with absolute agreement to assess intra-observer repeatability across three trials. The ICC value was 0.99 and indicates that the tissue depth measurements were strongly reliable.

The technical error of measurement (TEM) was calculated for each permutation of pairs of measurement error trials to assess intra-observer error using the following equation:

$$\text{TEM} = \sqrt{\frac{\sum D^2}{2N}}$$

where *D* is equal to the difference of measured values between two trials and *N* is equal to the number of individuals measured.[42] TEM values for each tissue depth measurement comparison are provided (Table 3). Overall mean TEM was 0.20mm and was considered adequately low for the purposes of this investigation.

After assessing reliability and TEM, tissue depths (Fig. 1) were measured by one investigator (JMS) on randomly ordered, coded and anonymized images on three separate occasions with at least 24 hours between each measurement session. Tissue depth measurements that differed by more than 1mm from homologous tissue depth values collected from the same individual were remeasured and replaced to minimize measurement error occurring from human error and imaging artifacts.

Individual tissue depth values for each side of the face were tested for normal distributions using a Kolmogorov-Smirnov test for normality and found to be normally distributed. A two-sample t-test was used to compare clefted and non-clefted sides of the face of males (n = 40) and females (n = 15). No statistical differences were detected between males and females (p-value = 0.43) and the samples were combined for analysis.

To carry out the asymmetry test the cleft and non-cleft side tissue depths were compared. A paired t-test was carried out to assess symmetry of tissue depths on each side of the face. A p-value of $\leq$ 0.05 was considered statistically significant for each test. With a type I error rate of 5% and a sample size of 55 individuals, this analysis has a 90% power to detect a difference of 0.09 mm between homologous tissue depths on the sides of the face.

Results

Several bilateral tissue depths exhibited significant asymmetry across the face (see table 4): frontal eminence (fe-fe', p-value = 0.012), lateral orbit (lo-lo', p-value = 0.016), nasal ala furrow (naf-naf', p-value = 0.013), subalare (sbl-sbl', p-value 0.003), mediolateral philtrum (p-value = 0.039), and lateral philtrum (p-value = 0.002). Tissue depths exhibiting significant asymmetry are depicted in Fig. 2.

One tissue depth on the forehead exhibited asymmetry, but this tissue depth was not near the location of the original cleft. The remaining tissue depths exhibited significant asymmetry and were localized to the midfacial region of the face where the congenital cleft originally occurred. Asymmetric tissue depths in the midfacial region were 0.6 – 1.6mm thicker on the side of the face where the cleft occurred.

Discussion

Symmetry of tissue depths in individuals with surgically repaired unilateral CL/P has rarely been investigated. Because individuals with CL/P undergo multiple surgical corrections that can include bone grafts and always include functional or aesthetic soft-tissue modifications it is important to understand whether the combination of the congential cleft and surgical interventions affect facial soft-tissue symmetry. We found that several tissue depths near the site of the congenital cleft exhibit significant asymmetry (Fig. 2). Tissue depths of the philtrum, cutaneous upper lip, and nose are 0.6 – 1.6 mm thicker on the side of the face where the congenital cleft occurred (Table 4). These differences are small, but might be clinically relevant because they contribute to overall facial asymmetry and stigmata. Development of soft tissue thickness upon the rest of the face appears to occur in a consistent and symmetric manner over the bony scaffold. Our results are comparable to those of Choi and colleagues who also found that unilateral CL/P soft tissue depths of the nasolabial regions are asymmetric and thicker on the clefted side of the face.[32]

One explanation for tissue depth asymmetry in CL/P faces is that the congenital cleft disrupts normal muscle formation and position by altering the length and insertion of nasolabial muscles.[40] Additionally, the congenital cleft frequently disrupts lateral incisor development on the clefted side of the face and alters symmetry of the maxillary bony scaffolds upon which soft tissue anchors itself.[29,32,43] Soft- and hard-tissue surgical corrections aimed at aesthetic and symmetric orofacial improvements attempt to correct facial deformities but may cause scarring and/or muscle pull that can induce anterioposterior and transverse asymmetries.[32]

Hall and Precious maintain that the nasal septum acts as a growth center or pacemaker for midfacial growth.[44] Congenital labiomaxillary clefts impair nasolabial muscle attachments on the clefted side of the nasal septum, which causes the nasal septum to deviate to one side of the face.[44] Ossification sites for the premaxilla and maxilla appear towards the end of the 6th week of gestation after the nasal capsule and facial muscle precursors are present, which means that asymmetric muscle forces already exist as osteogenesis shapes the midface.[44] Ultimately, midfacial growth becomes asymmetric, resulting in asymmetry of the nose, maxilla, and orbits.[44] These factors likely combine with those presented above to explain the tissue depth asymmetry found in this study.

One goal of surgeons who repair congenital craniofacial anomalies is to produce a harmonious and symmetric facial appearance.[40] The results of this study are clinically relevant because despite the best efforts of plastic surgeons to produce a symmetric and harmonious facial appearance there is usually residual facial asymmetry from CL/P that results in facial stigmata. Therefore, it is important to quantify facial asymmetry following cleft repair to determine how well surgeries restore facial harmony and symmetry, and thereby avoid qualitative and subjective assessments of facial form or surgical success.[40] Quantitative assessment and localization of asymmetry to particular facial regions is often challenging to plastic surgeons and orthodontists. CBCT images and the specialized measurement tools found in Dolphin imaging software allow precise tissue depth measurements to be collected to quantify soft-tissue craniofacial asymmetry and develop a treatment plan for the patient after evaluating the hard- and soft-

tissues of the craniofacial complex. These advanced techniques provide the surgeon with an accurate up-to-date image of hard and soft craniofacial tissues on the clefted and non-clefted sides of the face to reference when reconstructing the deformed facial regions. Since the differences in soft-tissue depths around the nose and mouth are small, although statistically significant, the surgeon should investigate hard tissue asymmetries in patients significant facial asymmetry.

In conclusion, the nasolabial, dentoalveolar, and orbital facial regions exhibit significant asymmetry of soft-tissue depths in patients born with unilateral CL/P. As expected, the philtrum shows the greatest asymmetry. Asymmetric tissue depths tend to be thicker on the clefted side of the face, possibly due to scarring and muscle pull. 3D imaging allows surgeons to precisely measure asymmetry in patients to increase the likelihood of successful surgical outcomes.

References

1. Manhein MH, Listi GA, Barsley RE, et al. In vivo facial tissue depth measurements for children and adults. *Journal of forensic sciences.* Jan 2000;45(1):48-60.

2. Dumont ER. Mid-facial tissue depths of white children: an aid in facial feature reconstruction. *Journal of forensic sciences.* Oct 1986;31(4):1463-1469.

3. Starbuck JM, Ward RE. The affect of tissue depth variation on craniofacial reconstructions. *Forensic science international.* Oct 25 2007;172(2-3):130-136.

4. Brugmann SA, Kim J, Helms JA. Looking different: understanding diversity in facial form. *American journal of medical genetics. Part A.* Dec 1 2006;140(23):2521-2529.

5. Burke PH, Hughes-Lawson CA. Developmental changes in the facial soft tissues. *American journal of physical anthropology.* Jul 1989;79(3):281-288.

6. Nanda R, Meng H, Kapila S, et al. Growth changes in the soft tissue facial profile. *The Angle orthodontist.* 1989;60(3):177-190.

7. Baume RM, Buschang PH, Weinstein S. Stature, head height, and growth of the vertical face. *American journal of orthodontics.* Jun 1983;83(6):477-484.

8. Farkas LG, Eiben OG, Sivkov S, et al. Anthropometric measurements of the facial framework in adulthood: age-related changes in eight age categories in 600 healthy white North Americans of European ancestry from 16 to 90 years of age. *The Journal of craniofacial surgery.* Mar 2004;15(2):288-298.

9. Farkas LG, Posnick JC. Growth and development of regional units in the head and face based on anthropometric measurements. *The Cleft palate-craniofacial journal : official publication of the American Cleft Palate-Craniofacial Association.* Jul 1992;29(4):301-302.

10. Farkas LG, Posnick JC, Hreczko TM. Growth patterns of the face: a morphometric study. *The Cleft palate-craniofacial journal : official publication of the American Cleft Palate-Craniofacial Association.* Jul 1992;29(4):308-315.

11. Farkas LG, Posnick JC, Hreczko TM, et al. Growth patterns of the nasolabial region: a morphometric study. *The Cleft palate-craniofacial journal : official publication of the American Cleft Palate-Craniofacial Association.* Jul 1992;29(4):318-324.

12. Farkas LG, Posnick JC, Hreczko TM, et al. Growth patterns in the orbital region: a morphometric study. *The Cleft palate-craniofacial journal : official publication of the American Cleft Palate-Craniofacial Association.* Jul 1992;29(4):315-318.

13. Neave R. Age changes in the face in adulthood. In: Clement J, Ranson D, eds. *Craniofacial identification in forensic medicine.* New York: CRC Press; 1998.

14. Thomason H, Dixon M. Craniofacial Defects and Cleft Lip and Palate. *Encyclopedia of Life Sciences (ELS).* Chichester: John Wiley & Sons; 2009.

15. Weinberg SM, Naidoo SD, Bardi KM, et al. Face shape of unaffected parents with cleft affected offspring: combining three-dimensional surface imaging and geometric morphometrics. *Orthodontics & craniofacial research.* Nov 2009;12(4):271-281.

16. Lee JK, Park JW, Kim YH, et al. Association between PAX9 single-nucleotide polymorphisms and nonsyndromic cleft lip with or without cleft palate. *The Journal of craniofacial surgery.* Sep 2012;23(5):1262-1266.

17. Hall BK, Precious DS. Cleft lip, nose, and palate: the nasal septum as the pacemaker for midfacial growth. *Oral surgery, oral medicine, oral pathology and oral radiology.* Sep 27 2012.

18. Bill J, Proff P, Bayerlein T, et al. Treatment of patients with cleft lip, alveolus and palate--a short outline of history and current interdisciplinary treatment approaches. *Journal of*

cranio-maxillo-facial surgery : official publication of the European Association for Cranio-Maxillo-Facial Surgery. Sep 2006;34 Suppl 2:17-21.

19. Boo-Chai K. An ancient Chinese text on a cleft lip. *Plastic and reconstructive surgery.* Aug 1966;38(2):89-91.

20. Rogers B, Grabb W, Rosenstein S, et al. History of cleft lip and palate treatment. *Grabb WC.* 1971.

21. Bugaighis I, Tiddeman B, Mattick CR, et al. 3D comparison of average faces in subjects with oral clefts. *European journal of orthodontics.* Nov 20 2012.

22. Freeman AK, Mercer NS, Roberts LM. Nasal asymmetry in unilateral cleft lip and palate. *Journal of plastic, reconstructive & aesthetic surgery : JPRAS.* Apr 2013;66(4):506-512.

23. Liu H, Warren DW, Drake AF, et al. Is nasal airway size a marker for susceptibility toward clefting? *The Cleft palate-craniofacial journal : official publication of the American Cleft Palate-Craniofacial Association.* Jul 1992;29(4):336-339.

24. Fukushiro AP, Trindade IE. Nasal airway dimensions of adults with cleft lip and palate: differences among cleft types. *The Cleft palate-craniofacial journal : official publication of the American Cleft Palate-Craniofacial Association.* Jul 2005;42(4):396-402.

25. Desalu I, Adeyemo W, Akintimoye M, et al. Airway and respiratory complications in children undergoing cleft lip and palate repair. *Ghana Medical Journal.* 2010;44(1):16-20.

26. Warren DW, Hairfield WM, Dalston ET, et al. Effects of cleft lip and palate on the nasal airway in children. *Archives of otolaryngology--head & neck surgery.* Sep 1988;114(9):987-992.

27. Hairfield WM, Warren DW, Seaton DL. Prevalence of mouthbreathing in cleft lip and palate. *The Cleft palate journal.* Apr 1988;25(2):135-138.

28. Gubisch W. Functional and aesthetic nasal reconstruction in unilateral CLP-deformity. *Facial plastic surgery : FPS.* Jul 1995;11(3):159-168.

29. Agarwal R, Parihar A, Mandhani PA, et al. Three-dimensional computed tomographic analysis of the maxilla in unilateral cleft lip and palate: implications for rhinoplasty. *The Journal of craniofacial surgery.* Sep 2012;23(5):1338-1342.

30. Nagasao T, Miyamoto J, Yasuda S, et al. An anatomical study of the three-dimensional structure of the nasal septum in patients with alveolar clefts and alveolar-palatal clefts. *Plastic and reconstructive surgery.* Jun 2008;121(6):2074-2083.

31. Weinberg SM, Brandon CA, McHenry TH, et al. Rethinking isolated cleft palate: evidence of occult lip defects in a subset of cases. *American journal of medical genetics. Part A.* Jul 1 2008;146A(13):1670-1675.

32. Choi YK, Park SB, Kim YI, et al. Three-dimensional evaluation of midfacial asymmetry in patients with nonsyndromic unilateral cleft lip and palate by cone-beam computed tomography. *Korean journal of orthodontics.* Jun 2013;43(3):113-119.

33. Wetmore RF. Importance of maintaining normal nasal function in the cleft palate patient. *The Cleft palate-craniofacial journal : official publication of the American Cleft Palate-Craniofacial Association.* Nov 1992;29(6):498-506.

34. Otero L, Bermudez L, Lizarraga K, et al. A comparative study of facial asymmetry in philippine, colombian, and ethiopian families with nonsyndromic cleft lip palate. *Plastic surgery international.* 2012;2012:580769.

35. Heliovaara A, Rautio J. Craniofacial cephalometric morphology in 6-year-old children with isolated cleft lip, isolated submucous cleft palate, and combined cleft lip and

submucous cleft palate. *Scandinavian journal of plastic and reconstructive surgery and hand surgery / Nordisk plastikkirurgisk forening [and] Nordisk klubb for handkirurgi.* 2007;41(2):53-58.

36. Williams EM, Evans CA, Reisberg DJ, et al. Nasal outcomes of presurgical nasal molding in complete unilateral cleft lip and palate. *International journal of dentistry.* 2012;2012:643896.

37. Bugaighis I, Mattick CR, Tiddeman B, et al. 3D asymmetry of operated children with oral clefts. *Orthodontics & craniofacial research.* Jul 15 2013.

38. Kane AA, DeLeon VB, Valeri C, et al. Preoperative osseous dysmorphology in unilateral complete cleft lip and palate: a quantitative analysis of computed tomography data. *Plastic and reconstructive surgery.* Apr 1 2007;119(4):1295-1301.

39. Seidenstricker-Kink LM, Becker DB, Govier DP, et al. Comparative osseous and soft tissue morphology following cleft lip repair. *The Cleft palate-craniofacial journal : official publication of the American Cleft Palate-Craniofacial Association.* Sep 2008;45(5):511-517.

40. Bell A, Lo TW, Brown D, et al. Three-Dimensional Assessment of Facial Appearance Following Surgical Repair of Unilateral Cleft Lip and Palate. *The Cleft palate-craniofacial journal : official publication of the American Cleft Palate-Craniofacial Association.* Jan 31 2013.

41. Olson EC, Miller RL. *Morphological Integration*. Chicago: University of Chicago Press; 1958.

42. Simpson E, Henneberg M. Variation in soft-tissue thicknesses on the human face and their relation to craniometric dimensions. *American journal of physical anthropology.* Jun 2002;118(2):121-133.

43. Jena AK, Singh SP, Utreja AK. Effects of sagittal maxillary growth hypoplasia severity on mandibular asymmetry in unilateral cleft lip and palate subjects. *The Angle orthodontist.* Sep 2011;81(5):872-877.

44. Hall BK, Precious DS. Cleft lip, nose, and palate: the nasal septum as the pacemaker for midfacial growth. *Oral surgery, oral medicine, oral pathology and oral radiology.* Apr 2013;115(4):442-447.

Table 1. Unilateral CL/P sample statistics.

Diagnosis	Total Sample size	Number of males	Number of females	Mean Age (yrs.) ± Standard Deviation	Age Range (yrs.)
Unilateral CL/P	55	40	15	11 ± 2.52	7-17

Table 2. Skeletal- and soft-tissue anatomical landmarks used to measure tissue depth on CBCT images.

Skeletal Landmarks	**Soft-Tissue Landmarks**
<u>Bilateral points</u>	<u>Bilateral points</u>
1. Frontal eminence (fe) - Bony projection of the ectocranial surface of the frontal bone.	1. Frontal eminence (fe') - The soft-tissue point directly overlying hard-tissue frontal eminence (fe).
2. Mid-Supraorbital (mso) - Centered superior margin of the orbit.	2. Mid-Supraorbital (mso') - The soft-tissue point directly overlying hard-tissue supraorbital (so).
3. Mid-Infraorbital (mio) - Centered inferior margin of the orbit.	3. Mid-Infraorbital (mio') - The soft-tissue point directly overlying hard-tissue infraorbital (io).
4. Lateral orbit (lo) - Center of the zygomatic process lined up with the lateral border of the orbit along the anterior-posterior axis.	4. Lateral orbit (lo') - The soft-tissue point directly overlying hard-tissue lateral orbit (lo).
5. Nasal Ala Furrow (naf) – Lateral border of the nasal aperture located directly underneath soft-tissue nasal ala furrow (naf').	5. Nasal Ala Furrow (naf') - Insertion of soft-tissue nasal ala furrow into lateral nose.
6. Subalare (sbal) - Inferior border of the nasal aperture located directly underneath soft-tissue subalare (sbal').	6. Subalare (sbal') – The point at the lower limit of each alar base, where the alar base disappears into the skin of the upper lip.
7. Mediolateral philtrum (mlp) – Point located where a sagittal line passes through the midpoint between the widest point of the nasal aperture and the anterior nasal spine and intersects with an axial line passing midway through the upper jaw above the teeth and below the inferior nasal aperture.	7. Mediolateral philtrum (mlp') – The soft-tissue point directly overlying hard-tissue mediolateral philtrum (mlp).
8. Lateral philtrum (lp) – Point located where a sagittal line passes through the widest point of the nasal aperture and intersects with an axial line passing midway through the upper jaw above the teeth and below the inferior nasal aperture.	8. Lateral philtrum (lp) – The soft-tissue point directly overlying hard-tissue lateral philtrum (lp).
9. Zygion (zy) - The most lateral point of the zygomatic arch.	9. Zygion (zy') - The soft-tissue point directly overlying hard-tissue zygomatic arch (za).
10. Supraglenoid (sgl) - Root of the zygomatic arch just before the ear.	10. Supraglenoid (sgl') - The soft-tissue point directly overlying hard-tissue supraglenoid (sg).
11. Gonion (go) - Point located on the jaw line at the level of the angle between the posterior and the inferior borders of the mandible.	11. Gonion (go') - The soft-tissue point directly overlying hard-tissue gonion (go).
12. Supra M^1 (sm^1) - Point located on the alveolar process at the level of the middle of the first upper molar.	12. Supra M^1 (sm^1') - The soft-tissue point directly overlying hard-tissue supra m^1 (sm^1).
13. Occlusal line (ol) - Point located on anterior margin of the ramus of the mandible, in alignment with the plane of dental occlusion.	13. Occlusal line (ol') - The soft-tissue point directly overlying hard-tissue occlusal line (ol).
14. Infra M_1 (im_1) - Point located on the alveolar process at the level of the middle of the first lower molar.	14. Infra M_1 (im_1') - The soft-tissue point directly overlying hard-tissue infra m_1 (im_1).

Table 3. Technical error of measurement (TEM) across each permutation of the three measurement trials.

Lateral Tissue Depths (mm)	fe-fe'	mso-mso'	mio-mio'	lo-lo'	naf-naf'	sbal-sbal'	mlp-mlp'	lp-lp'	zy-zy'	sgl-sgl'	go-go'	sm1-sm1'	ol-ol'	im1-im1'
TEM trial 1 vs. trial 2	0.22	0.17	0.22	0.25	0.17	0.21	0.12	0.13	0.14	0.22	0.19	0.21	0.24	0.37
TEM trial 2 vs. trial 3	0.20	0.13	0.15	0.31	0.19	0.16	0.12	0.14	0.12	0.28	0.19	0.29	0.17	0.24
TEM trial 1 vs. trial 3	0.18	0.17	0.20	0.19	0.14	0.19	0.11	0.12	0.10	0.18	0.17	0.29	0.32	0.35
Mean TEM	0.20	0.16	0.19	0.25	0.17	0.18	0.12	0.13	0.12	0.23	0.18	0.27	0.24	0.32
Overall Mean TEM = 0.20mm														

Table 4. Tissue depths exhibiting significant asymmetry (mm). The left side represents the side of the face with the congenital cleft for each measurement.

	Mean (mm)	S.D. (mm)
Left frontal eminence (lfe-lfe')	5.012	1.346
Right frontal eminence (rfe-rfe')	5.357	1.722
Difference	-0.345	0.866
95% CI for mean difference: (-0.611, -0.079)		
P-value = 0.012		
Left lateral orbit (llo-llo')	14.259	2.62
Right lateral orbit (rlo-rlo')	13.638	3.128
Difference	0.621	1.627
95% CI for mean difference: (0.12, 1.122)		
P-value = 0.016		
Left nasal ala furrow (lnaf-lnaf')	15.359	3.741
Right nasal ala furrow (rnaf-rnaf')	14.239	3.423
Difference	1.12	2.84
95% CI for mean difference: (0.246, 1.994)		
P-value = 0.013		
Left subalare (lsbal-lsbal')	14.543	2.903
Right subalare (rsbal-rsbal')	13.533	2.829
Difference	1.01	2.089
95% CI for mean difference: (0.367, 1.653)		
P-value = 0.003		
Left mediolateral philtrum (lmlp-lmlp')	12.965	2.819
Right mediolateral philtrum (rmlp-rmlp')	11.86	3.302
Difference	0.705	3.221
95% CI for mean difference: (0.287, 1.696)		
P-value = 0.039		
Left lateral philtrum (llp-llp')	14.935	2.985
Right lateral philtrum (rlp-rlp')	13.378	3.153
Difference	1.557	3.058
95% CI for mean difference: (0.616, 2.499)		
P-value = 0.002		
* S.D. – Standard Deviation		

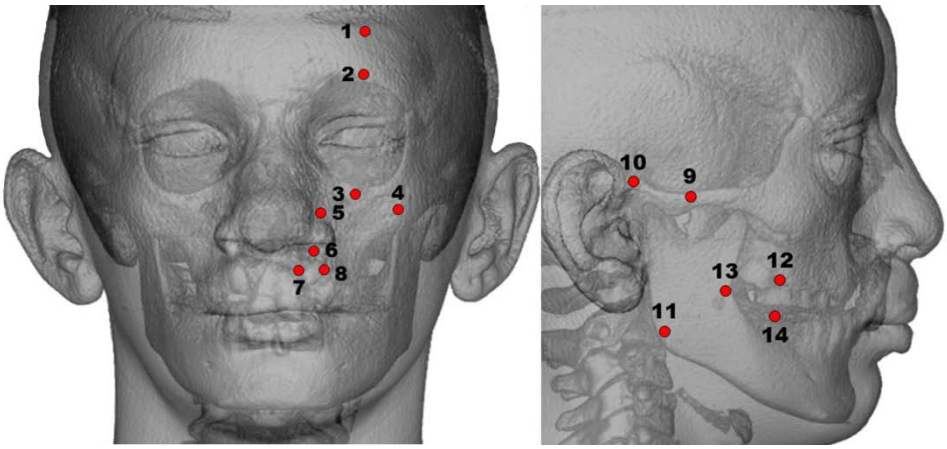

Figure 1. Tissue depth locations measured on CBCT images. Dolphin software was used to automatically calculate the distances between the hard and soft-tissue anatomical landmarks.

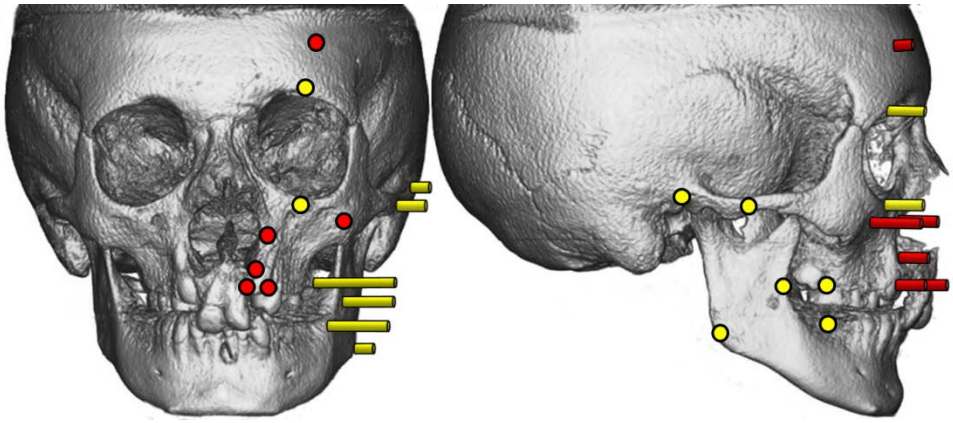

Figure 2. Tissue depth asymmetry. Tissue depths that exhibit significant asymmetry are depicted in red and names are listed in Table 4. Tissue depths depicted in yellow are not significantly different. The majority of tissue depths that are asymmetric are localized to the midfacial region near the location of the congenital cleft.